Effect of the Interelectronic Repulsion on the Information Content of Position and Momentum Atomic Densities

J. C. ANGULO,[1,2] S. LÓPEZ-ROSA,[1,2] J. ANTOLÍN[2,3]

[1]*Departamento de Física Atómica, Molecular y Nuclear, Universidad de Granada, 18071 Granada, Spain*
[2]*Instituto* Carlos I *de Física Teórica y Computacional, Universidad de Granada, 18071 Granada, Spain*
[3]*Departamento de Física Aplicada, EUITIZ, Universidad de Zaragoza, 50018 Zaragoza, Spain*

Received 3 March 2009; accepted 16 April 2009
Published online 13 October 2009 in Wiley InterScience (www.interscience.wiley.com).
DOI 10.1002/qua.22317

ABSTRACT: The interelectronic repulsion is strongly responsible of the main structural characteristics of the atomic densities and, in particular, of their level of information content. In this work, the effect of such a repulsion on some information-theoretic descriptors is quantified and analyzed by considering different complexities and distances between the Bare Coulomb Field (BCF) and the Hartree–Fock (HF) position and momentum densities of neutral atoms throughout the Periodic Table. In doing so, the Quantum Similarity Index (QSI), the Quadratic Distance (QD), the Jensen-Shannon (JSD) and Fisher (FD) Divergences as well as complexity measures are employed. Int J Quantum Chem 110: 1738–1747, 2010

Key words: atomic one-particle densities; interelectronic repulsion; Jensen-Shannon and Fisher divergences; quantum similarity index; quadratic distance

1. Introduction

The interelectronic repulsion within atomic systems forbides to consider the global atom as a nucleus "surrounded" by a mere superposition of one-electron orbitals, each one governed exclusively by the electron-nucleus attraction potential which depth being given by the nuclear charge Z. Ignoring the repulsive forces is the basic feature of the so-called Bare Coulomb Field (BCF) model [1] among others, in which the electron densities in both position and momentum spaces are determined by adding over all orbitals the corresponding hydrogen-like densities.

This work deals with the problem of quantifying the disimilarity among atomic electron densities built up within different models, in order to establish a comparison to be interpreted according to the main differences between both the models. Especially interesting appears the case in which the

Correspondence to: J. C. Angulo; e-mail: angulo@ugr.es
Contract grant sponsor: Spanish MICINN.
Contract grant numbers: FIS-2008-02380, FIS-2005-06237, FQM-2445, P05-FQM-00481, and P06-FQM-01735.

interelectronic repulsive force is taking into account in one model but not in the other, with the aim of analyzing the most relevant informational characteristics, as will be described later, of the respective one-particle densities.

Different choices of models involving or not the repulsion can be considered. Such is the case, for instance, of the BCF model in the "non-repulsive" case, but not the only one. At this point, it is worthy to remark the well-known Kohn–Sham equations and the associated densities [2], where the Fermi statistics between the spin-like electrons remains performing the appropriate manipulations. This framework, together with some additional models, will be also considered elsewhere with similar and complementary aims. For the main purposes of this work, the quantitative comparisons between atomic densities are carried out taking as reference "non-repulsive" densities the BCF ones. Similar comments concerning atomic densities arising from equations enclosing the repulsive terms can be also done, in the sense that different frameworks are susceptible of being employed, such as the Near-Hartree–Fock with or without relativistic corrections, configuration interaction, etc.

Some results have been rigorously proved concerning BCF densities. For instance, March showed that the electron charge density is a monotonically decreasing function for an arbitrary number of closed shells in the BCF case [1], and also the same property holds in the momentum space [3]. Additional results for the kinetic and total energies have been also obtained [4–6]. More recently computations for the atomic reciprocal form factor have been carried out in a BCF showing that this relevant quantity is spherically symmetric, positive and monotonically decreasing [7], and also more general mathematical results have been also provided [8].

Instead of considering the BCF problem and solutions, more sophisticated models, such as the Hartree–Fock (HF) one [2], appear necessary in order to properly describe the atomic system by also considering the repulsive forces among electrons. Thinking on the N electron density in position space as a negatively charged cloud located around the nucleus with positive charge Z, it is immediate to realize that the interelectronic repulsion makes the cloud to increase its spread over the whole space and to decrease the mean speed of its constituents. This effect has an influence on the position and momentum atomic electron densities when taking into account the repulsive forces when compared with those built up from the purely attractive electron-nucleus potential. In this sense, it should be expected the repulsion to give rise, on one hand, to a more sparse position density and, on the other hand, to a momentum density more concentrated around the origin as center of the region of very low speeds.

The aforementioned intuitive notions on the effects of the repulsive forces among electrons on their representative one-particle densities in both position and momentum spaces would be desirable to be described not only qualitatively, as just done above, but also quantitatively by means of appropriate density functionals in order to quantify the specific level of sparsing of both the BCF (non-repulsive) and the HF (including repulsion) densities, and also by measuring in an appropriate way the 'distance' between both the models in terms of the corresponding distributions.

Different ways of measuring the information content of a distribution as well as the distance between two of them have been succesfully applied in many diverse fields [9–14], physics and chemistry among them and, in particular, in the study of atomic systems [15–21]. As a first step, the spreading degree of a given normalized-to-unity density function $\rho(\mathbf{r})$ can be measured by means of well-known information-theoretic functionals, such as the Shannon entropy [22],

$$S_\rho \equiv -\int \rho(\mathbf{r}) \ln \rho(\mathbf{r}) d\mathbf{r}, \tag{1}$$

the Fisher information [23]

$$I_\rho \equiv \int \rho(\mathbf{r}) |\vec{\nabla} \ln \rho(\mathbf{r})|^2 d\mathbf{r}, \tag{2}$$

the disequilibrium [24–27]

$$D_\rho \equiv \int \rho^2(\mathbf{r}) d\mathbf{r} \tag{3}$$

or the variance,

$$V_\rho \equiv \langle r^2 \rangle - \langle r \rangle^2 \tag{4}$$

($\langle r^k \rangle$ being the kth-order radial expectation value of the density), among others. It is worthy to remark here that Fisher information I_ρ posseses a "local character," in the sense of its value being very sensitive to strong changes of the density even within very small regions, contrary to the "global character" of the others measures defined above, which are much more dependent on the shape of the distribution over its whole domain.

In spite of the information provided by those functionals, a more complete description usually requires to deal with magnitudes involving more than a unique descriptor of the aforementioned ones, as is the case of the so-called complexities, being specially relevant the product-like ones such as the LMC [24], the Fisher–Shannon [28], and the Cramer–Rao [29] complexities. These quantities are proposed as general indicators of pattern, structure, and correlation, revealing also how far from the extreme cases (highly concentrated functions approaching a Dirac delta, and almost uniform ones everywhere) the density is. The limiting cases correspond to very low values of any complexity, for which one of their constituent factors (according to the extreme case considered) reaches its minimal value as well as the complexity itself.

Appart from quantifying the absolute information of a single distribution, it also appears very interesting to have at our disposal multiple-density functionals in order to measure the distance and/or similarity among them. This kind of measures have been commonly employed to establish how distant is the distribution we are interested in from a given "a priori" one usually chosen by following a criteria according to the specific poblem we are dealing with. Again, there appear different definitions of "distance," each one displaying its own properties, which makes it more or less appropriate depending on the specific characteristics of the distributions that are more interesting to be compared. Let us mention here, as relevant distance measures, the Quantum Similarity Index (QSI) [30, 31] and the Quadratic Distance (QD), both defined in terms of overlap integrals of the distributions, as well as the Fisher (FD) [32] and Jensen–Shannon (JSD) [13, 33, 34] divergences, which definitions are based, respectively, on the concepts of relative Fisher information [35, 36] and Kullback–Leibler or relative Shannon entropy [14, 37].

It is worthy to point out that the aforementioned "global" or "local" character of different information functionals also translates on the associated complexities and distances defined in terms of them. Consequently, the local character is only displayed by the Fisher Divergence FD, the other distances being of global character, and similarly concerning complexities according to being or not defined in terms of Fisher information I_ρ.

The main aim of this work is to study the effect of the interelectronic repulsions on all neutral atoms throughout the Periodic Table by means of their electron densities $\rho(\mathbf{r})$ and $\gamma(\mathbf{p})$ in both conjugated spaces, namely position and momentum, respectively. In doing so, the aforementioned information functionals and/or distances will be considered within the Bare Coulomb Field and the Hartree–Fock models. For the systems we are dealing with, i.e., neutral atoms in the absence of external fields, it is sufficient to consider the spherically averaged densities $\rho(r)$ and $\gamma(p)$. The results in both spaces will be analyze from a physical point of view according to relevant structural characteristics of the atomic densities, such as the shell-filling process. The BCF densities are easily built up in terms of hydrogen-like wavefunctions, whereas the numerical study throughout this work in the HF case will be carried out by using the accurate Near-Hartree–Fock wavefunctions of Koga et al. [38].

2. The Quantum Similarity Index (QSI) and the Quadratic Distance (QD)

The concept of "distance" between distributions finds its roots in the same concept associated to a coupled of elements in a vectorial space, constituing in fact an extension of it. Supplying an appropriate norm on the space in such a way of giving rise to a metric or distance leads us to the best known and deeply studied L^2 space, in which the distance between two vectors is given by the square root of the scalar product of the difference vector with itself. Considering the space of finite norm distributions defined over the whole three-dimensional space, and normalizing properly, the quadratic distance, to be denoted by QD, is defined as

$$\mathrm{QD}(\rho_1, \rho_2) \equiv \left\{ \int [\rho_1(\mathbf{r}) - \rho_2(\mathbf{r})]^2 d\mathbf{r} \right\}^{1/2} \qquad (5)$$

Among all well-known properties any distance has, let us remark that (i) it is non-negative for any pair of distributions, and (ii) the minimal value zero is reached if and only if both functions are identical (supossed to be defined both over the same domain). Having these properties in mind, it is clear that the QD values provide us with an indicator of similarity between densities. Nevertheless, it is not at all the only one. In this sense, it is worthy to remark here the definition of the so-called Quantum Similarity Index (QSI) [39, 40], given in terms of exactly the

same three integrals as for the QD after carrying out the squaring operation, which is given by

$$\mathrm{QSI}(\rho_1, \rho_2) \equiv \frac{\int \rho_1(\mathbf{r})\rho_2(\mathbf{r})d\mathbf{r}}{\sqrt{\int \rho_1^2(\mathbf{r})d\mathbf{r} \int \rho_2^2(\mathbf{r})d\mathbf{r}}} \tag{6}$$

where the numerator is referred as the "Quantum Similarity Measure" (QSM) of ρ_1 and ρ_2, whereas the denominator is defined in terms of the corresponding disequilibriums defined in Eq. (3). The main properties of this measure, appart from symmetry, are (i) it ranges over the bounded interval $[0, 1]$ and (ii) the maximal value 1 is only reached for the identical case. Its definition arises from the molecular research field [30], but later on has been widely applied in many different problems and subjects in order to establish a comparative measure as indicator of "similarity" between both distributions taking the base of the aforementioned main properties [41–45]. Let us remark here the different character of both measures in spite of being defined in terms of exactly the same integrals, attending to the boundeness of the QSI contrary to the unbounding property of QD. This comment can be also expressed in terms of the "saturation" values (those corresponding to identical distributions), being 0 for QD and 1 for QSI.

Let us numerically analyze both measures (QD and QSI) between the BCF and HF electron densities, in position and momentum spaces, $\rho(r)$ and $\gamma(p)$, respectively. In Fig. 1(a), $\mathrm{QD}_r(\mathrm{HF}, \mathrm{BCF})$ is displayed for all neutral atoms with nuclear charge $Z = 1-103$, and similarly in Fig. 1(b) for the momentum space (by only replacing the HF and BCF densities ρ by γ and, consequently, the variable "r" by "p"). First, we can observe that the values in both figures have been drawn as piecewise curves, each piece corresponding to the periods, which constitute the periodic table. This has been made in order to better interpret the results according to the shell-filling process. As should be expected, increasing the number of electrons makes the distance between both the models also to increase, due to the higher effect of the electronic repulsion, as clearly observed in Fig. 1(a).

In spite of the piecewise drawing procedure, the curve in Fig. 1(a) corresponding to $\mathrm{QD}_r(\mathrm{HF}, \mathrm{BCF})$ appears almost continuous while $\mathrm{QD}_p(\mathrm{HF}, \mathrm{BCF})$ in Fig. 1(b) clearly displays the aforementioned piecewise behavior attending to the periods the atoms belong to. Nevertheless, the periodicity pattern can be also observed in $\mathrm{QD}_r(\mathrm{HF}, \mathrm{BCF})$, not in terms of apparent discontinuities in the curve as occurs in

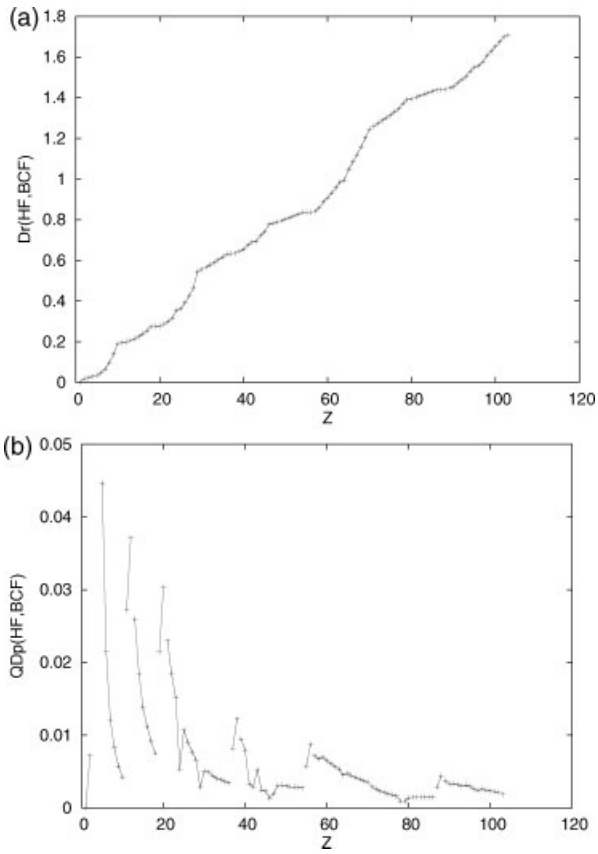

FIGURE 1. Quadratic Distance QD(HF, BCF) for neutral atoms with nuclear charge $Z = 1 - 103$ in (a) position and (b) momentum spaces. Atomic units are used.

momentum space, but as changes in its slope when going from a period to the next one. These results are interpreted as follows: the main characteristic which share both models is the identical value of the nuclear charge Z, and also that the region around the nucleus is mainly governed by the attractive electron-nucleus potential over the repulsive one. The last one is dominant over the first in external regions (valence subshell), which characterizes the periodicity patterns of the atomic systems. However, the rapid decrease (exponential) of the charge densities makes the external subshells contribution to the integrals to be almost negligible. The opposite can be argued in discussing Fig. 1(b), where more slow electrons (close to $p = 0$) are just those of valence subshells which, consequently, carry a relevant apport on computing the integrals. These comments can be better understood by observing Figs. 2(a) and (b), where the involved one dimensional integrands (the functions integrated from 0 to ∞) are

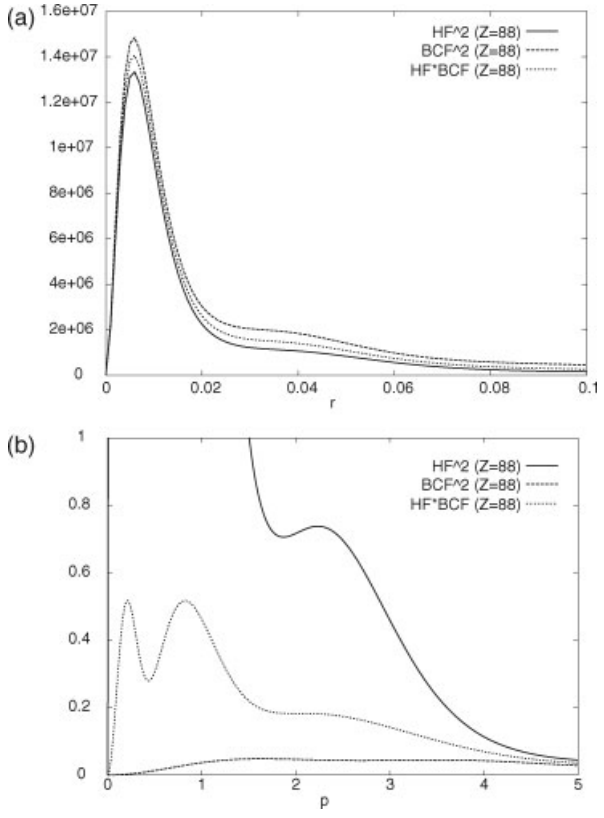

FIGURE 2. (a) Functions $4\pi r^2 \rho^2_{\mathrm{HF}}(r)$ (label HF^2), $4\pi r^2 \rho^2_{\mathrm{BCF}}(r)$ (label BCF^2), and $4\pi r^2 \rho_{\mathrm{HF}}(r)\rho_{\mathrm{BCF}}(r)$ (label HF*BCF), defining overlap integrals for computing the Quadratic Distance $\mathrm{QD}_r(\mathrm{HF}, \mathrm{BCF})$ for $Z = 88$ atom in position space, and (b) similarly in momentum space for the Quadratic Distance $\mathrm{QD}_p(\mathrm{HF}, \mathrm{BCF})$ of momentum densities $\gamma(p)$. Atomic units are used.

represented in order to appreciate their contribution to the global integrals. As previously mentioned, it is clearly observed that the relevant values of the three involved integral in position space, even for heavy atoms [$Z = 88$ as in Fig. 2(a)] are strongly localized very close to the origin (i.e., the nucleus) displaying there almost identical values, whereas the differences among them in momentum space for the same atom [Fig. 2(b)] are not only much stronger but also displayed over a much wider region.

A similar analysis is also carried out in terms of similarities QSI between the BCF and HF densities in both conjugated spaces. This is done attending to Fig. 3, where QSI(HF, BCF) are displayed again for $Z = 1 - 103$ in position and momentum spaces [Fig. 3(a)]. It is clearly observed that values of similarity between both models in position space are extremely close to the maximal value 1 and appear to be very little sensitive to the specific valence subshell of the considered systems, contrary to the momentum space case, which have a decreasing trend and showing, additionally, the shell-filling patterns including the anomalous cases. Justifying these results requires again the previous interpretation concerning the quadratic distance QD attending to the behavior of the involved integrals. Nevertheless, it is possible to observe the aforementioned structural characteristics also in position space by restricting ourselves to a much narrower interval for QSI_r(HF,BCF), as shown in Fig. 3(b) for values all above 0.975. From the analysis of both figures, it is worthy to point out that, in spite of QSI displaying periodicity patterns in both conjugated spaces, the position one appears to posseses a much smaller sensitivity in this sense than the momentum one.

It is worthy to point out that location of extrema in both QD and QSI in momentum space mostly belongs to noble gases ($Z = 10, 18, 36, 54, 86$) or

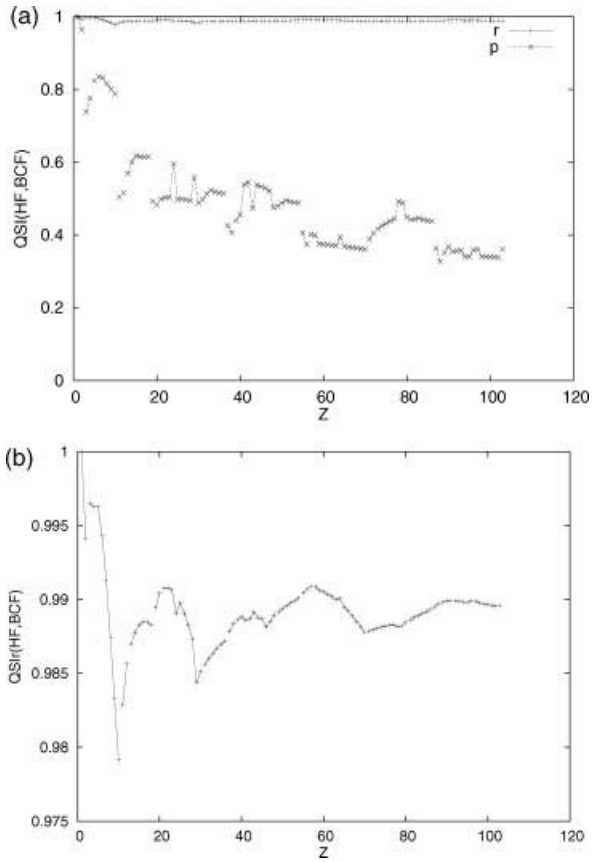

FIGURE 3. Quantum similarity index QSI(HF, BCF) for neutral atoms with nuclear charge $Z = 1 - 103$ in position and momentum spaces. Atomic units are used.

atoms suffering anomalous shell-filling (e.g., $Z = 24, 29, 46, 64, 79, 93$), usually minima for QD being maxima for QSI.

Summarizing the results of the present section, it has been clearly shown that distances based on overlap integrals as QD and QSI in order to quantify the effects of the interelectronic repulsion in atomic systems are mainly determined by the nuclear charge Z in position space, displaying much richer information on shell structure when dealing with momentum space densities.

3. The Fisher (FD) and Jensen–Shannon (JSD) Divergences

Apart from the above-discussed distances defined in terms of overlap integrals, there also exist additional comparative measures, some of them arising at a first step from fundamental information-theoretic functionals of a single distribution, such as Shannon entropy [Eq. (1)] and Fisher information [Eq. (2)], and their later extensions for establishing information-based comparisons among distributions, as is the case of the Kullback–Leibler relative entropy [14] and the relative Fisher information [35, 36].

To preserve the desirable properties of any distance measure, namely non-negativity, symmetry, and saturation for identical distributions, the aforementioned relative Shannon and Fisher measures give rise to their associated concept of "divergence." Both them are defined as follows: the Fisher Divergence (FD) is defined as the symmetrized Fisher relative entropy, given by

$$\mathrm{FD}(\rho_1, \rho_2) \equiv \int \rho_1(\mathbf{r}) \left| \vec{\nabla} \ln \frac{\rho_1(\mathbf{r})}{\rho_2(\mathbf{r})} \right|^2 d\mathbf{r} + \int \rho_2(\mathbf{r}) \left| \vec{\nabla} \ln \frac{\rho_2(\mathbf{r})}{\rho_1(\mathbf{r})} \right|^2 d\mathbf{r} \quad (7)$$

and similarly for the Jensen–Shannon Divergence (JSD) in terms of the Kullback–Leibler entropy (KL),

$$\mathrm{KL}(\rho_1, \rho_2) \equiv \int \rho_1(\mathbf{r}) \ln \frac{\rho_1(\mathbf{r})}{\rho_2(\mathbf{r})} d\mathbf{r} \quad (8)$$

where JSD is the sum of KL distances of each density to the mean one, namely

$$\mathrm{JSD}(\rho_1, \rho_2) \equiv \mathrm{KL}\left(\rho_1, \frac{\rho_1 + \rho_2}{2}\right) + \mathrm{KL}\left(\rho_2, \frac{\rho_1 + \rho_2}{2}\right), \quad (9)$$

equivalently expressed, after minor manipulations, in terms of Shannon entropies as

$$\mathrm{JSD}(\rho_1, \rho_2) \equiv S\left(\frac{\rho_1 + \rho_2}{2}\right) - \frac{1}{2}[S(\rho_1) + S(\rho_2)], \quad (10)$$

being consequently interpreted as the "excess" of Shannon entropy of the mean density respect to the mean value of the individual Shannon entropies. From their definitions, the aforementioned properties of distance measures are immediately observed to be verified, where non-negativity of JSD arises from the convex character of Shannon entropy S or the non-negativity of KL. So both JSD and FD divergences provide us with comparative measures of the distance between two distributions, each one based on a relevant descriptor of the information content. Such a distance character of the JSD and the FD divergences has been previously employed in studying different systems, problems, and/or processes [32, 43, 46].

Let us now apply these concepts of distance to the previously afforded problem of comparing the BCF and HF atomic densities in position and momentum spaces, in order to quantify the effect of the electronic repulsion on the information content of the densities as well as on the periodicity patterns. This will be done by analyzing Figs. 4(a), (b), and 5 in which the aforementioned divergences are represented for neutral atoms throughout the whole Periodic Table.

The Fisher Divergence FD(HF, BCF) is displayed in Figs. 4(a) (position space) and 4(b) (momentum space, in log-scale). Similarly to the previously studied quantities (Section 2), monotonicity characters are opposite in both spaces, displaying an increasing behavior in position space and decreasing in the momentum one. Again, the overall behavior in each space is the expected one in the sense of a higher number of electrons making more relevant the repulsive effect and expanding the charge cloud. Nevertheless, now shell-filling patterns can be clearly appreciated in both conjugated spaces, whereas QSI and QD values appeared to be related to such a process only in momentum space. In what concerns location of extrema, most of them correpond (as also ocurred with momentum space QD

and QSI) to noble gases or anomalous shell-filling cases, maxima in position space corresponding to minima in the the momentum one and conversely.

Concerning the Jensen–Shannon Divergence JSD (HF,BCF) represented in Fig. 5 for both conjugated spaces, some comments are in order. First, the shell-filling process of the atomic systems is also revealed in the position and the momentum spaces, both curves displaying a very similar shape. In fact, they differ roughly in a scaling factor and/or a small shift depending on the range of Z values considered (light, medium, or heavy atoms). Nevertheless, the difference between the absolute values of JSD_r and JSD_p for a given Z are much smaller than for all previously studied measures, some of them even belonging to different magnitude orders. Again location of extrema corresponds mostly to noble gases and anomalous shell-filling systems, but now being of the same type (minimum or maximum) in both conjugated spaces, contrary to the opposite character for the FD_r and FD_p divergences.

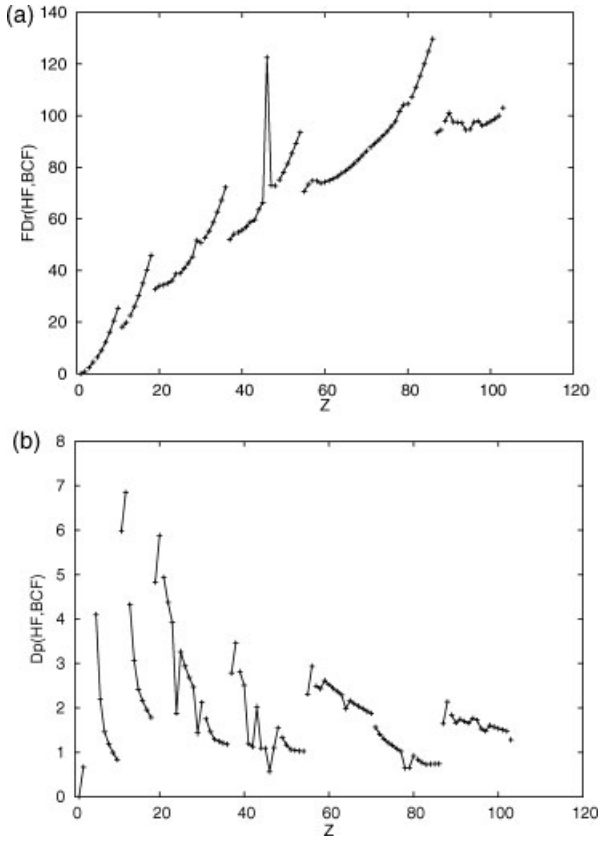

FIGURE 4. Fisher Divergence FD(HF, BCF) for neutral atoms with nuclear charge $Z = 1 - 103$ in (a) position and (b) momentum spaces. Atomic units are used.

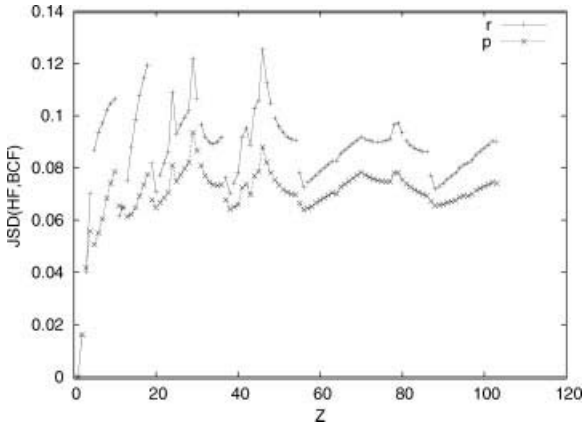

FIGURE 5. Jensen–Shannon Divergence JSD(HF, BCF) for neutral atoms with nuclear charge $Z = 1 - 103$ in position and momentum spaces. Atomic units are used.

So, it is clearly shown that the Fisher (FD) and Jensen–Shannon (JSD) Divergences are the most useful measures, when compared with the others considered in this work, in order to study the inter-electronic repulsion effects by means of position space densities, but similar results are also provided by the same quantities in the momentum space.

4. Complexity Measures

Different meanings appear associated to a global concept of "complexity," which constitutes a measure of structure and correlation in systems and processes. This is the reason of finding many definitions [24, 47–52] of complexity as well as several fields of application [53–56]. Nevertheless, information concepts such as entropy, disequilibrium, and others also studied in this work are usually basic ingredients in its quantification, which is not unique appearing strongly conditioned according to the specific system or process under study.

Most proposals of formulating this quantity build it up as the product of two factors [57–59], being not the only way of defining it. One factor takes into account order/disequilibrium and the other disorder/uncertainty. Their product gives rise to the complexity, which provides a measure of how far the distribution is from the extremum cases of maximum localization or maximum disorder for which complexity reaches minimal values.

Among the more succesful definitions for studying different kind of problems such as those afforded

in this work, it is worthy to remark the following ones, for which some rigorous results have been also provided: (i) the López–Ruiz, Mancini and Calbet complexity (CLMC) [24], (ii) the Fisher–Shannon complexity (CFS) [28], and (iii) the Cramer–Rao complexity (CCR) [29]. Deep additional studies of the associated information planes substended by the constituent factors have been also carried out [60, 61].

The CLMC complexity CLMC(ρ) is defined in terms of the so-called exponential entropy $L \equiv e^S$ (S being the Shannon entropy) and the disequilibrium D as defined by Eq. (3), being given by their product [57]

$$\mathrm{CLMC}(\rho) \equiv e^{S_\rho} \cdot D_\rho \tag{11}$$

with S quantifying the uncertainty and D the level of order. The way of defining this magnitude arises from the appropriate scaling and replication properties desirable for such a measure of information.

Concerning the Fisher–Shannon complexity CFS(ρ), it is formulated as the product of Fisher information I_ρ and the so-called power entropy J_ρ as [28]

$$\mathrm{CFS}(\rho) \equiv I_\rho \cdot J_\rho \tag{12}$$

with

$$J_\rho \equiv \frac{1}{2\pi e} e^{\frac{2}{3}S_\rho}, \tag{13}$$

while the Cramer–Rao complexity replaces the Shannon-based delocalization factor by the variance V_ρ defined in Eq. (4), giving rise to [29]

$$\mathrm{CCR}(\rho) \equiv I_\rho \cdot V_\rho \tag{14}$$

The usefulness of the CLMC complexity and some of its extensions and generalizations has been widely shown [54, 55, 57], as well as the recently introduced CFS [29] and CCR [62] complexities, particularly for the study in atomic and molecular physics [15–17, 31, 63–65] giving rise to new insights in this field from an information-theoretic point of view. Nevertheless, they have been usually employed with the aim of providing information on multielectronic systems by computing their complexities within an specific model (e.g., Hartree–Fock among others), but not for comparing their values from different models in order to interpret their differences according to relevant physical properties, such as the interelectronic repulsion as in this job.

For illustration, let us compare the CLMC complexity values of the HF and BCF systems in both position and momentum spaces, as displayed, respectively, in Figs. 6(a) and (b). As expected from the intuitive notion of complexity described above, such an information measure increases when the system is not only governed by the attractive potential (BCF), but additionally by the repulsive interelectronic one (HF). Such an increase is strongly dependent on the atomic shell-structure, the BCF curves containing much slighter peaks (local extrema) when compared with those of the HF values. This different level of structure is observed in both conjugated spaces, more enhanced in the momentum one. Location of extrema are usually associated (as ocurred with previously studied measures) to noble gases and anomalous shell-filling, their character (maximum or minimum) being conditioned by the considered space (position or momentum) and system (HF or BCF). Similar comments can be also done concerning Fisher–Shannon and Cramer–Rao complexities, CFS, and CCR, respectively, whose associated figures are not shown for the sake of shortness.

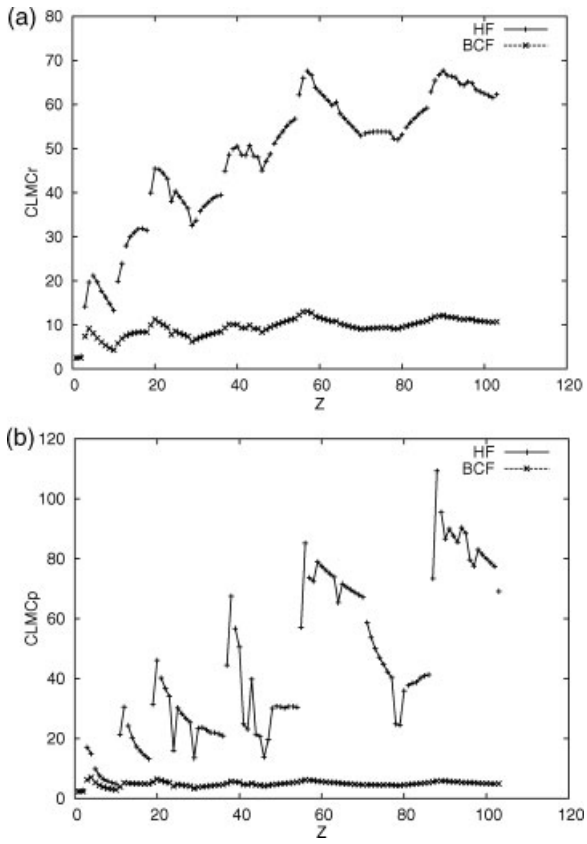

FIGURE 6. LMC complexity measures CLMC(HF) and CLMC(BCF) for neutral atoms with nuclear charge $Z = 1 - 103$ in (a) position and (b) momentum spaces. Atomic units are used.

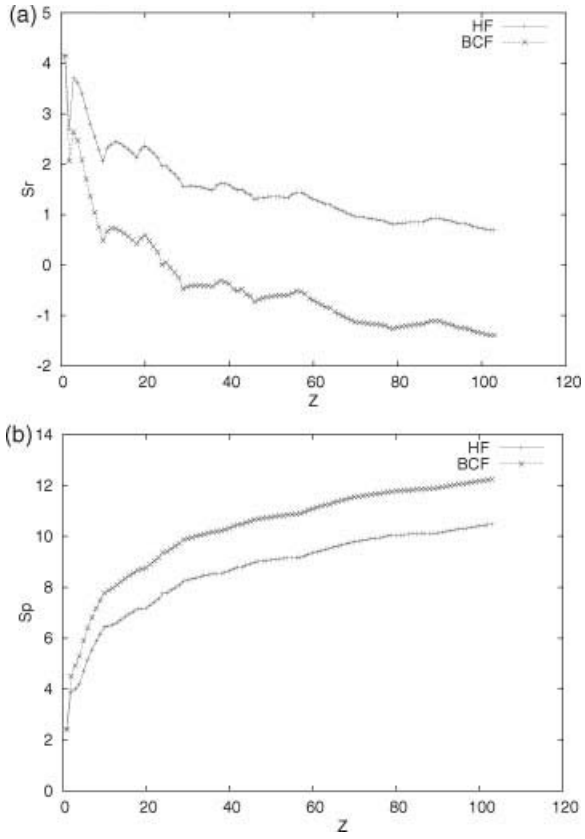

FIGURE 7. Shannon entropies S(HF) and S(BCF) for neutral atoms with nuclear charge $Z = 1 - 103$ in (a) position and (b) momentum spaces. Atomic units are used.

It is natural to wonder to which extent the aforementioned complexities provide a complete informational description of the differences between the BCF and HF systems according to both the electron repulsion effect and the shell-filling process. This can be clearly appreciated by studying Figs. 7(a) and (b), corresponding to the Shannon entropies $S(HF)$ and $S(BCF)$ in position and momentum spaces, respectively, and comparing them to the previously analyzed CLMC complexities. Let us keep in mind that one of the CLMC factors is essentially the Shannon entropy (its exponential in fact). In spite of the Shannon entropy appearing shifted attending to the inclusion or not of the repulsive forces, it is not quite enough to display by itself the relevant sructure associated to shell-filling, as does occur with LMC complexity. In fact, both HF and BCF Shannon entropies in momentum space are monotonically increasing functions (without local extrema). These observations enhance the previously mentioned main feature of complexity as information measure, appearing able to provide much richer information than the individual factors composing it. These comments can be also applied to the study of the other considered CFS and CCR complexities and their factors.

5. Conclusions

The study of different distribution distances, divergences, and complexities allows to gain a deeper physical insight on the relevance of the interlectronic repulsion in atomic systems as compared with the corresponding purely Coulombic ones. To obtain a complete informational description, it appears preferable to deal simultaneously with measures in position and momentum atomic densities. Nevertheless, Fisher and Jensen-Shannon divergences as well as complexities provide relevant information in both conjugated spaces, whereas distances based on overlap integrals necessarily requieres to employ momentum densities. Appart from the repulsion effect, the shell-filling patterns in the HF framework are also clearly displayed in the just mentioned cases, not only attending to the specific valence subshell but additionally to its occupation number, the information measures detecting also the anomalous shell-filling.

References

1. March, N. H. Phys Rev A 1986, 33, 88.
2. Parr, R. G.; Yang, W. Density-Functional Theory of Atoms and Molecules; Oxford University Press: Oxford, 1989.
3. Smith, V. H., Jr.; Robertson, D. D.; Tripathi, A. N. Phys Rev A 1990, 42, 61.
4. March, N. H.; Santamaría, R. Phys Rev A 1989, 39, 2835.
5. Howard, I. A.; March, N. H. J Phys A 2002, 35, L635.
6. March, N. H.; Cizek, J. Int J Quantum Chem 1988, 33, 301.
7. Angulo, J. C.; Romera, E. Int J Quantum Chem 2006, 106, 485.
8. Lin, C.; Lin, M. Comm Nonlinear Sci Numer Simul 2008, 12, 677.
9. Cover, T. M.; Thomas, J. A. Elements of Information Theory; Wiley-Interscience: New York, 1991.
10. Renyi, A. In Proceedings of the 4th Berkeley Symposium on Mathematics, Statistics and Probability, 1960; pp 547–561.
11. Tsallis, C. J Statis Phys 1988, 52, 479.
12. Pearson, K. Phil Mag 2000, 50, 157.
13. Taneja, I. J.; Pardo, L.; Morales, D.; Menéndez, M. L. Questiio 1989, 13, 47.
14. Kullback, S.; Leibler, A. Ann Math Statist 1951, 22, 79.
15. Gadre, S. R.; Bendale, R. D. Phys Rev A 1987, 36, 1932.

16. Guevara, N. L.; Sagar, R. P.; Esquivel, R. O. Phys Rev A 2003, 67, 012507.
17. Nalewajsky, R. F. Information Theory of Molecular Systems; Elsevier Science: Boston, 2006.
18. Angulo, J. C. Phys Rev A 1994, 50, 311.
19. Ho, M.; Smith, V. H., Jr.; Weaver, D. F.; Gatti, C.; Sagar, R. P.; Esquivel, R. O. J Chem Phys 1998, 108, 5469.
20. Borgoo, A.; Godefroid, M.; Indelicato, P; De Proft, F.; Geerlings, P. J Chem Phys 2007, 126, 44102.
21. Liu, S. J Chem Phys 2007, 126, 191107.
22. Shannon, C. E.; Weaver, W. The Mathematical Theory of Communication; University of Illinois Press: Urbana, 1949.
23. Fisher, R. A. Proc Cambridge Philos Soc, 1925, 22, 700.
24. López-Ruiz, R.; Mancini, H. L.; Calbet, X. Phys Lett A 1995, 209, 321.
25. Onicescu, O. CR Acad Sci Paris A 1966, 263, 25.
26. Pipek, J.; Varga, I. Phys Rev A 1992, 46, 3148.
27. Carbó-Dorca, R.; Arnau, J.; Leyda, L. Int J Quantum Chem 1980, 17, 1185.
28. Angulo, J. C.; Antolín, J.; Sen, K. D. Phys Lett A 2008, 372, 670.
29. Angulo, J. C.; Antolín, J. J Chem Phys 2008, 128, 164109.
30. Carbó-Dorca, R.; Girones, X.; Mezey, P. G., Eds. Fundamentals of Molecular Similarity; Kluwer Academic/Plenum Press: New York, 2001.
31. Nalewajski, R. F.; Parr, R. G. Proc Natl Acad Sci USA 2000, 97, 8879.
32. Antolín, J.; Angulo, J. C.; López-Rosa, S. J Chem Phys 209, 130, 074110.
33. Lin, J. IEEE Trans Inform Theory 1991, 37, 145.
34. Taneja, I. J. In Advances in Electronics and Electron Physics; Hawkes, P. W., Ed.; Academic Press: London, 1989; pp 327–413.
35. Hammad, P. Revue de Statistique Appliquée 1978, 26, 73.
36. Biane, P.; Speicher, R. Annales de l'Institut Henri Poincare (B) Probability and Statistics 2001, 37, 581.
37. Janssens, S.; Borgoo, A.; van Alsenoy, C.; Geerlings, P. J Phys Chem A 2008, 112, 10560.
38. Koga, T.; Kanayama, K.; Watanabe, S.; Thakkar, A. J. Int J Quantum Chem 1999, 71, 491.
39. Solá, M.; Mestres, J.; Oliva, J. M.; Durán, M.; Carbó-Dorca, R. Int J Quantum Chem 1996, 58, 361.
40. Robert, D.; Carbó-Dorca, R. Int J Quantum Chem 2000, 77, 685.
41. Borgoo, A.; Godefroid, M.; Sen, K. D.; de Proft, F.; Geerlings, P. Chem Phys Lett 2004, 399, 363.
42. Borgoo, A.; Torrent-Sucarrat, M.; de Proft, F.; Geerlings, P. J Chem Phys 2007, 126, 234104.
43. Ho, M.; Sagar, R. P.; Schmider, H.; Weaver, D. F.; Smith, V. H., Jr. Int J Quantum Chem 1995, 53, 627.
44. Angulo, J. C.; Antolín, J. J Chem Phys 2007, 126, 044106.
45. Antolín, J.; Angulo, J. C. Eur Phys J D 2008, 46, 21.
46. de Proft, F.; Ayers, P. W.; Sen, K. D.; Geerlings, P. J Chem Phys 2004, 120, 9969.
47. Kolmogorov, A. N. Probl Inf Transm 1965, 1, 3.
48. Chaitin, G. J ACM 1966, 13, 547.
49. Lempel, A.; Ziv, J. IEEE Trans Inform Theory 1976, 22, 75.
50. Grassberger, P. Int J Theor Phys 1986, 25, 907.
51. Bennet, C. H. In The Universal Turing Machine—A Half Century; Herhen, R., Ed.; Oxford University Press: Oxford, 1988; pp 227–257.
52. Lloyd, S.; Pagels, H. Ann Phys (NY) 1988, 188, 186.
53. Shalizi, C. R.; Shalizi, K. L.; Haslinger, R. Phys Rev Lett 2004, 93, 118701.
54. Rosso, O. A.; Martin, M. T.; Plastino, A. Physica A 2003, 320, 497.
55. Chatzisavvas, K. Ch.; Moustakidis, CH. C.; Panos, C. P. J Chem Phys 2005, 123, 174111.
56. Lamberti, P. W.; Martin, M. T.; Plastino, A.; Rosso, O. A. Physica A 2004, 334, 119.
57. Yamano, T. J Math Phys 2004, 45, 1974.
58. Shiner, J. S.; Davison, M.; Landsberg, P. T. Phys Rev E 1999, 59, 1459.
59. López-Ruiz, R. Biophys Chem 2005, 115, 215.
60. Sen, K. D.; Antolín, J.; Angulo, J. C. Phys Rev A 2007, 76, 032502.
61. Antolín, J.; Angulo, J. C. Int J Quantum Chem 2009, 109, 586.
62. Dehesa, J. S.; Sánchez-Moreno, P.; Yáñez, R. J. J Comput Appl Math 2006, 186, 523.
63. Borgoo, A.; De Proft, F.; Geerlings, P.; Sen, K. D. Chem Phys Lett 2007, 444, 186.
64. Sen, K. D.; Panos, C. P.; Chatzisavvas, K. Ch.; Moustakidis, Ch. C. Phys Lett A 2007, 364, 286.
65. Panos, C. P.; Chatzisavvas, K. Ch.; Moustakidis, Ch. C.; Kyrkou, E. G. Phys Lett A 2007, 363, 78.